Long Term Morphological Changes after Construction

In the model simulations Gaps 1 and 2 were closed at the end of 2006, and morphological simulations carried out for a further 10 years (i.e. to 2016) to predict post-construction long-term changes in the sea bed.

With the completion of the sea dike and the subsequent closure of the three gaps, the tideland area is separated from the tidal flow which leads to the formation of a lake. The bed shear stress induced by the tide is therefore negligible in the inshore area. The bed shear stress is also low to the south-west of Gap 1, to the west of Gap 2 (in the deeper water) and outside Gap 3 (as in 2003). Changes in the tidal currents further offshore have increased the bed shear stress in the area around the offshore islands.

Figure 13 shows the initial rate of bed level change immediately following the closure of Gaps 1 and 2, and highlights limited erosional / depositional activity in the area of the sea dike. Note that the scale of the rates of bed level change are an order of magnitude lower than those in the corresponding figures when the Gaps were open. At this reduced plotting scale there is a region of activity around the mouth of the River Geum and also around the islands shown outside the sea dike.

The predicted bed changes from 2006 to 2016 are shown in Figure 17, and conform with the patterns of erosion and deposition shown in Figure 16. Over the 10 years simulation period seabed level changes of up to 5m are predicted to occur in the areas between the islands, although the actual morphological changes in these areas will depend strongly on the nature of the seabed.

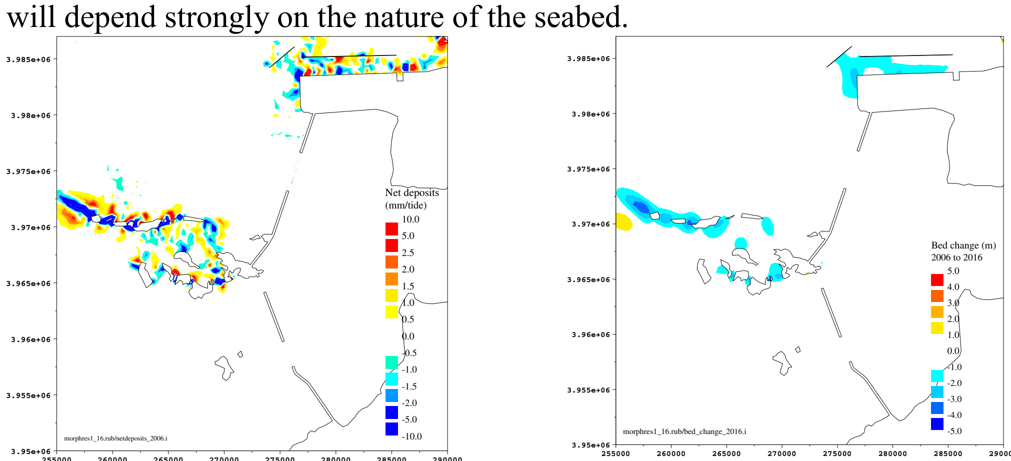

Figure 16. Initial rates of bed level change following closure of all gaps (left), and predicted bed changes in the study area 2006 to 2016 (right)

Following closure of the sea dike the morphology of the tideland will be modified by locally generated wave action which will tend to redistribute the sediment, eroding it from the higher areas and depositing it into the deeper areas. In addition, the will be a net influx of material from the Mangyeong and Dongjin Rivers.

SENSITIVITY TESTING ON FLUVIAL FLOWS

The study area is fed by the Dongjin and Mangyeong Rivers. To the north of the tidal reclamation area, the Geum River discharges into the study area. Fluvial information provided by RRI was used to perform sensitivity tests to consider the importance of the freshwater discharge on the sediment transport and morphology of the study area. TELEMAC-2D was run for spring tide conditions with peak river discharges relating to each of the above rivers of $250m^3/s$, $900m^3/s$ and $3500m^3/s$ respectively. The ensuing hydrodynamic field was fed into SANDFLOW, and the results were analysed. This sensitivity test concluded that although the morphological activity was affected as a consequence of these high discharge events, the sediment transport is dominated by the tidal filling and emptying of the site. Over the timescales considered it was concluded that the fluvial input has a negligible effect on the morphological evolution. Following complete closure, however, the sediment load in the Dongjin and Mangyeong Rivers will have a controlling influence on the tideland morphology in the very long term.

CONCLUSIONS AND DISCUSSION

During the sea dike construction (i.e. up to 2006) bed level changes occur rapidly, with net erosion rates reaching up to 3m/year and net deposition occurring at up to 1m/year. During the construction simulation, Gap 3 was closed at the end of 2003 and the associated change in the hydrodynamics leads to a significant change in the distribution and magnitude of the rate of bed evolution. Following complete closure of the sea dike the longer term post construction morphological changes (i.e. from 2006 to 2016) are largely confined to the offshore areas, around the islands to the west of the sea dike.

Figure 18 shows the predicted changes in the bed level over the entire study period between 2001 and 2016. The primary change is one of net erosion which occurs in the region of the gap locations, a connecting channel between Gap 3 and 2 on the landward side of the sea dike, and a deepening of the existing channel between Gaps 1 and 2 and inshore. There are a few regions of net deposition, notably to the west of each of the gaps (and greatest offshore of Gap 2) where eroded material held in suspension settles, and also within the tideland inshore of each of the gaps.

A comment on the degree of accuracy of the morphological predictions is appropriate. It should be borne in mind that sediment transport prediction is not an exact science, not least because the physical processes that give rise to the entrainment, transport and settling of sediment are not fully understood. Long term predictions of morphology are subject to a large degree of uncertainty for the same reasons but also because there is uncertainty in the occurrence of natural processes (e.g. storm events) that may play a role in the evolution. Equally, it should be appreciated that the modelling has made further assumptions including that the seabed comprises sediments that are able to be eroded by the extent predicted: should there be limited deposits with stronger sediment or rock below the surface this will limit the morphological evolution. In addition, the sensitivity tests highlighted the strong variability in the sediment transport predictions according to the sediment grain size. Given that the site is characterised by mixed sediments, and also that the sea dike will have an influence on the characteristics of the seabed deposits through an increase in sedimentation of fine material trapped within the tideland, the actual seabed evolution may differ to that simulated.

Accordingly it is considered that the predictions of morphology change are a credible representation of the potential change that could occur over the periods simulated, but that the actual changes that occur may differ somewhat due to various reasons including those given above. It should also be appreciated, however, that the magnitude of the predicted morphological changes in the simulations are comparable with those that occurred from 1987 to 2001 which serves to add credibility to the results.

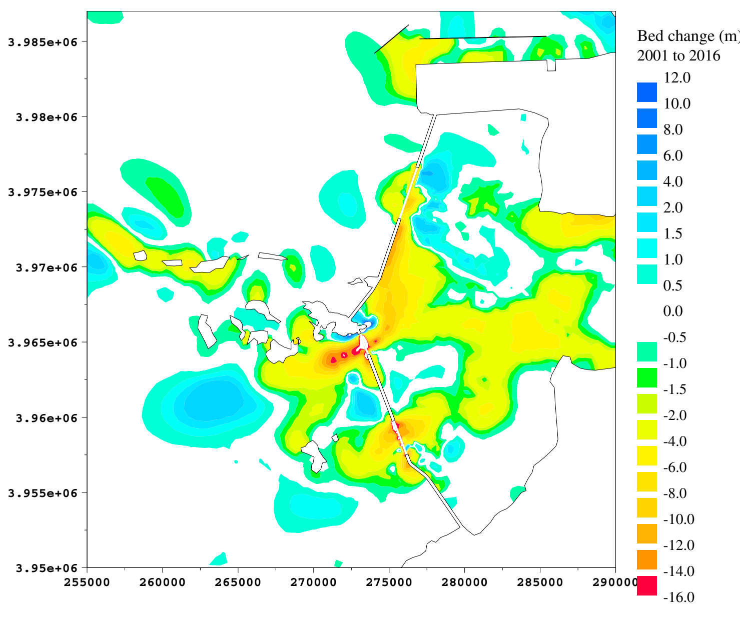

Figure 18. Predicted bed changes in the study area 2001 to 2016

ACKNOWLEDGEMENTS
The authors gratefully acknowledge the helpful assistance of RRI, Korea during the course of this project.

REFERENCES

Chesher TJ and Miles GV (1992). The concept of a single representative wave for sediment transport predictions. In Falconer, R. A., Chandler-Wilde, S. N. and Liu, S. Q. (editors) (1992) Hydraulic and Environmental Modelling: Coastal Waters. *Proceedings on Hydraulic and Environmental Modelling of Coastal, Estuarine and River Waters*. Ashgate Publishing Limited.

De Vriend HJ, Capobianco M, Chesher TJ, De Swart HE, Latteux B, Stive MJF (1993). Approaches to Long-term Modelling of Coastal Morphology: A Review. *Coastal Engineering*, 21 (1993) 225-269

MORPHOLOGICAL MODELLING OF ARTIFICIAL SAND RIDGE NEAR HOEK VAN HOLLAND, THE NETHERLANDS

L.C. van Rijn, D.J.R. Walstra and P.K. Tonnon

Delft Hydraulics, P.O. Box 177, 2700 MH Delft, The Netherlands. leo.vanrijn@wldelft.nl

Abstract: The study is focussed on the morphological modelling (based on DELFT3D model) of an artificial sand rige at the Dutch shoreface near Hoek van Holland close to the harbour of Rotterdam. The ridge is perpendicular to the coast and to the tidal flow. The sediment size is about 0.3 mm. The tidal range is about 2 m. The peak flood velocities (to north) and ebb velocities (to south) are about 0.6 and 0.55 m/s. Using a 1DH (depth-averaged) model approach, the growth and migration of a sand ridge can not be simulated properly as the modification of the velocity profiles can not be represented. This latter effect can only be simulated by using a 2DV (two-dimensional vertical) or a 3D model approach. Growth of the sand ridge can occur when bed-load transport is dominant. Decay (flattening) of the ridge occurs when suspended load transport is dominant, particularly when waves are important.

INTRODUCTION

From 1982 to 1986 dumpings of sand at the shoreface near Hoek van Holland (close to entrance of harbour of Rotterdam) created an artificial sand ridge, known as sand ridge Hoek van Holland, with a length of about 3600 m normal to the peak tidal current and the shore (location Hoek van Holland, see Figure 1A) in an area with depths between 15 m and 23 m on the northern side of the approach channel to harbour of Rotterdam. In all, 3.5 million m^3 sand was dumped over the period 1981 to 1986 (Van Woudenberg, 1996). The ridge dimensions just after creation of the ridge were: length of about 3600 m; toe width between 250 m and 370 m; height between 1.3 and 4 m; slopes between 1:50 and 1:100 on the south flank and between 1:20 and 1:50 on the north flank; d_{50} between 0.15 mm and 0.45 mm. The landward end of the ridge is about 6300 m from the shoreline. The sand ridge Hoek van Holland is located close to Loswal Noord, which is a dumping site for mud from the Rotterdam harbour basins. The ridge is perpendicular to the coast and to the tidal flow. Primary goals were to study the stability of this submerged ridge, normal to the tidal flow and to study the effect of the ridge on the sand transport at the shoreface.

Figure 1B shows a schematic plan view of the sounding area and sections; the sections are 400 m apart. The width of the sounding area is about 2100 m. Section 1 is about 6 km from the coast. In this study the attention is focussed on the modelling of Section 3 using the DELFT3D model in line and in area mode (1DH, 2DV, 2DH and 3D). Details of the modelling of other sections are given by Tonnon (2005).

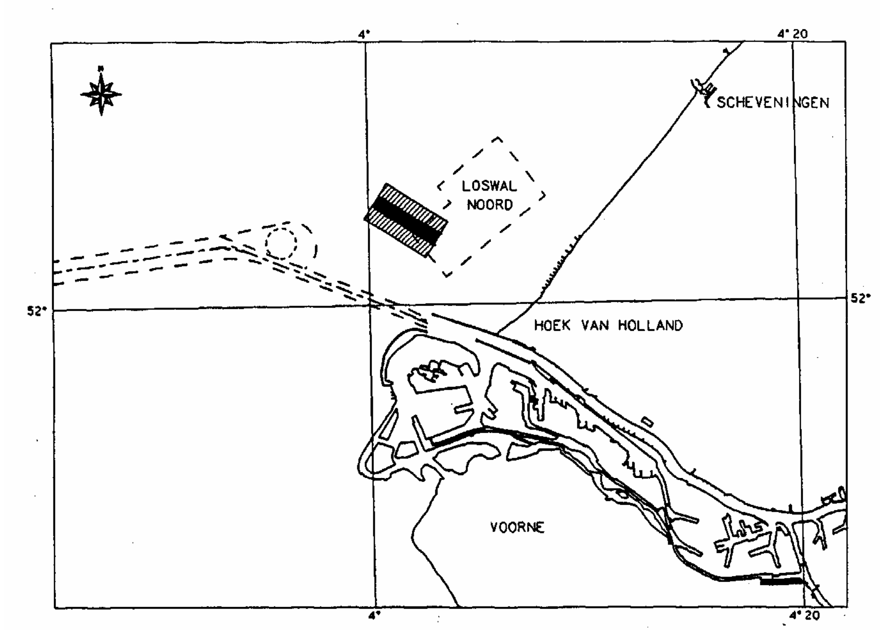

Figure 1A. Location sand ridge Hoek van Holland.

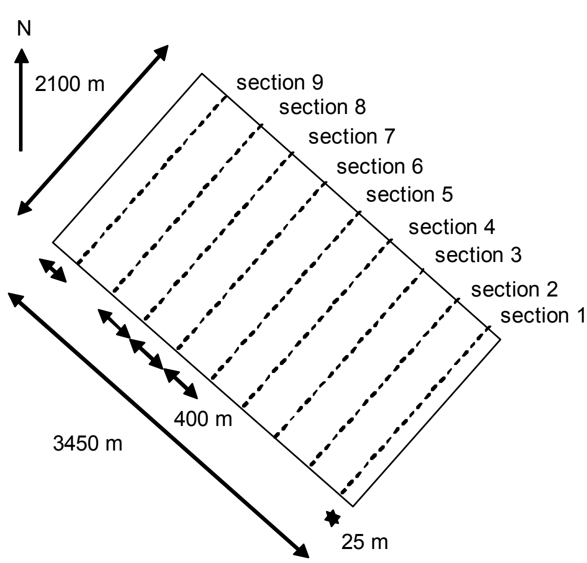

Figure 1B. Schematic plan view of the sounding area and sections

ANALYSIS OF BATHYMETRY DATA

Since 1982 yearly bathymetric surveys were carried out by Directorate North Sea (DNZ) of Rijkswaterstaat. Soundings before 1991 were not available on tape and were digitized from maps or microfilm, and thus are less reliable. Data collection before 1991 was carried out with the less-accurate single beam method, while data collection after 1991 was carried out with the more accurate multi-beam method. Soundings were carried out based on fixed tide gauges at Hoek van Holland; using this data an amplitude correction was carried out.

Two datasets were obtained, the first spanning the period 1982 to 1997, the second covering the period 1991 to 2000. Comparison of the two datasets shows that the second dataset (1991 to 2000) is somewhat out of line with the first (1982 to 1997), as the z-values are about 0.1 to 0.15 m lower.

The morphological development of the ridge is shown (1982, 1991, 1995 and 2000) for cross-sections 3 and 4, see Figure 2.

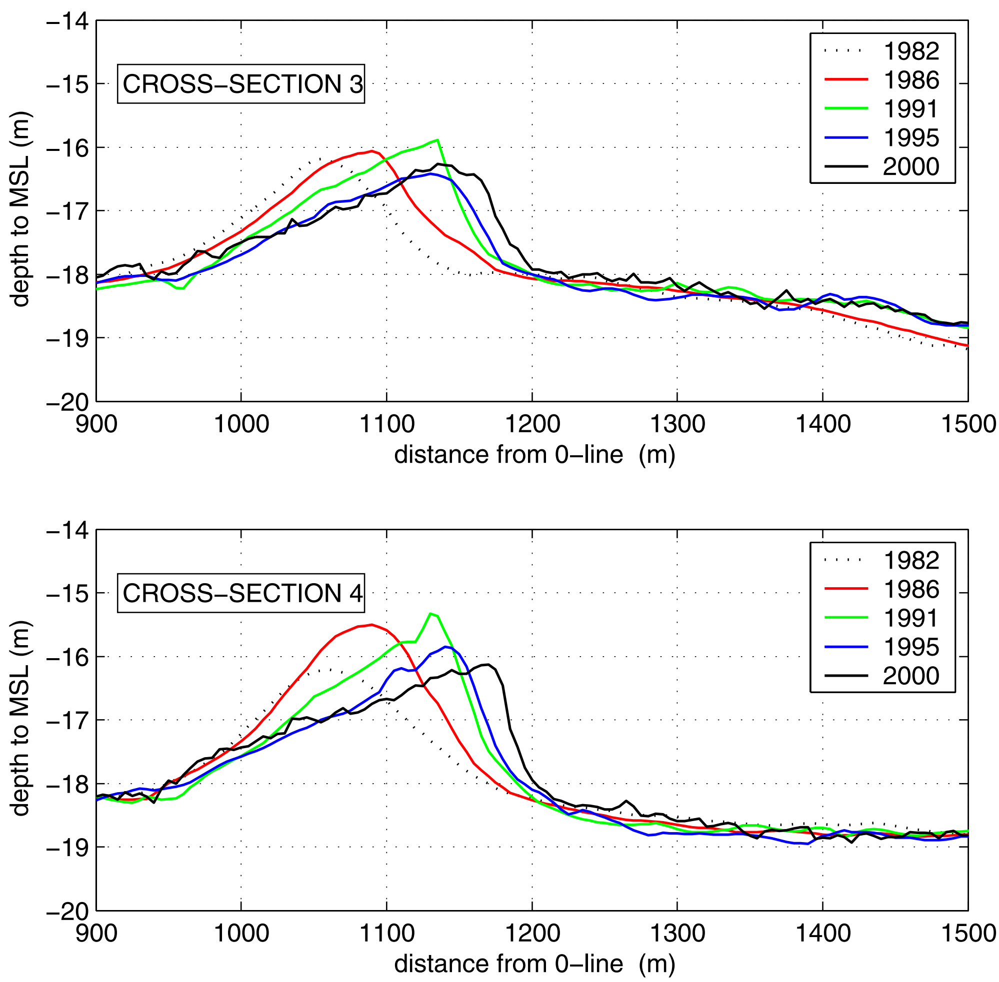

Figure 2. Measured bed level developments for Sections 3 and 4.

Analysis of the soundings between 1982 and 2000 shows a clear reduction of the ridge height in time and a net migration of the ridge in flood direction to the north. The rate of migration reduces with increasing depth. The average migration of crest of the ridge in northern direction is about 5.50 m per year and the average decrease in height is about 0.1 m per year. Between 1992 and 1993 a southward migration of the ridge and increase in height were observed. From sedimentation and erosion volumes it was found that overall, between 1982 and 2000, more sediment was eroded at the southern side of the ridge than accreted at the northern side of the ridge; hence, sediment was lost from the study area. However, between 1986 and 1999 a net gain of sediment was observed in the study area. Between 1991 and 2000 sediment was lost from the study area. Sedimentation/erosion plots show annually changing patterns per year with, on average, erosion taking place at the top of the ridge and sedimentation directly north of the ridge.

MODELS USED

The DELFT3D modelling system developed by WL | Delft Hydraulics has been used to simulate the morphological processes. It can simulate flows, waves, sediment transport and morphological developments. The modelling system consists of several modules. Herein, a short description is given of FLOW and WAVE. Using the DELFT3D-WAVE module, the evolution of wind-generated waves can be simulated. The WAVE module is either based on HISWA or SWAN; SWAN, an acronym for Simulating Waves Nearshore, is a third generation, spectral wave model that computes the non-steady propagation of short crested waves over an uneven bottom, considering wind action, dissipation due to bottom friction, wave-breaking, refraction, shoaling and directional spreading. The SWAN model takes into account the following physics: wave propagation in time and space, shoaling due to current and depth, refraction and frequency shifting; wave generation by wind; dissipation by white-capping, depth-induced breaking and bottom friction; non-linear wave-wave interactions; wave-induced set-up; wave-blocking by flow. The wave conditions (i.e. wave forces based on the energy dissipation rate or the radiation stresses, orbital velocities) calculated in DELFT3D-WAVE module are used as input for the DELFT3D-FLOW module, to compute wave-driven currents, enhanced turbulence, bed-shear stress and stirring up by wave breaking. Herein, SWAN has not been used, but a constant wave height in the computational domain has been used.

The FLOW-module is a hydrodynamic simulation program, which calculates non-steady flow and transport phenomena resulting from tidal and/or meteorological forcing on a curvilinear, boundary fitted grid. The numerical system of the program solves the unsteady shallow water equations in two or three dimensions. Typical applications of DELFT3D-FLOW includes simulations of tide and wind driven flows, stratified and density driven flows, river flow, transport of dissolved material and pollutants.

The shallow water equations are based on the three-dimensional Navier-Stokes equations for incompressible free surface flow, under the assumption of shallow water and Bousinesq. In the vertical momentum equation the vertical accelerations are neglected, which lead to the hydrostatic pressure equation. The system of partial differential equations for conservation of mass and momentum is solved with a finite difference method on the model grids.

The sediment-online module is an add-on with the DELFT3D-FLOW module which concerns simultaneous computation of flows and transports and simultaneous feedback to bottom changes. This module was recently updated based on the TR2004 sand transport formulations (Van Rijn et al. 2004). The most important improvements involve a bed-roughness predictor for the previously user-specified current-related and wave-related bed roughness parameters and a refined predictor for the suspended sediment size. The reference concentration of the suspended sediment concentration profile was recalibrated. The hydronamic flow calculations are always carried out using the correct bathymetry. Morphodynamic developments take place on a time scale several times longer than typical flow changes, leading to long simulation times in case of morphological predictions. To shorten the simulation time, a morphological time scale factor can be used, whereby the speed of the changes in the morphology is scaled up to a rate where it begins to have a significant impact on the hydrodynamic flows.
DELFT3D uses a sigma-coordinate system for the vertical grid, whereby the vertical grid consists of layers bounded by two sigma planes, which are not strictly horizontal but follow the bottom topography and the free surface. As a result a smooth representation of the topography is obtained. For a sigma coordinate grid the number of layers is constant over the entire horizontal computational area, irrespective of the water depth. The distribution of the relative layer thickness is usually non-uniform. This allows for more resolution in the zones of interest such as the near surface area (important for e.g. wind-driven flows) and the near bed area (sediment transport). Due to the use of a sigma coordinate grid, only the number of layers and relative thickness of each layer has to be specified. Herein, a vertical grid of 20 computational layers with a logarithmic layer distribution and a relative bottom layer thickness of 2% of the water depth is used.

MODEL RUNS FOR IDEALIZED RIDGE SCHEMATIZATION

The idealized sand ridge consists of a symmetric ridge (sediment size of d_{50}=0.3 mm; d_{90}=0.6 mm) at a depth comparable to the actual sand ridge near Hoek van Holland. A symmetric Gaussian-shaped sand ridge was created for the simulations, which roughly resembles the ridge characteristics at Sections 3 and 4 in 1991 (Fig. 2), i.e. a mean depth outside the ridge of about -17.8 m to MSL, a ridge height of about 3 m and a ridge width of about 400 m. The formula which was used to create the Gaussian shape reads:

$$z_b = H \cdot \exp(-x^2 / L^2) \qquad (1)$$

with L being the e-folding distance in x-direction over which the height decreases with a factor 1/e, and H being the height of the ridge. Here, L is taken as 100 m and H is taken as 3 m, the top of the ridge is located at 1150 m from the first boundary. The tidal flow is represented by a sinusoidal function ($U=U_0+U_1\cos(\omega t)$; $h=h_0+\zeta\cos(\omega t)$) with and without a net current (drift U_0), thus representing a propagating tidal wave as in the Dutch coastal zone. Phase differences between horizontal and vertical tides are not taken into account. These simulations were carried out to gain insight in the physical processes at the sand ridge and to study the effect of tides, waves and basic model settings on the morphological development (over 5 years) of an idealized sand ridge. To reduce the computational time, the numerical simulations are run over a much shorter period of 273 hours; the morphological changes are speed up to that of the 5 year period using a morphological scale factor. The simulation period of 273 hours includes a spin-up period of 33 hours to allow the model to adapt itself to the boundary conditions. During the spin-up period no bed level updating takes place; the effective simulation time is therefore 240 hours, in this period 20 complete tidal cycles of 12 hours are simulated. The physical parameters used are: Coriolis acceleration set up for 52 °N; acceleration of gravity set to 9.81 m/s^2; air density set to 1.000 kg/m^3; water density set to 1025 kg/m^3; salinity set to 31 ppt and water temperature set to 15 °C.

A spationally constant wave height was used. The effects of four different wave conditions were studied: H_s = 1.50 m, T_p=5.0 s, direction 315 °N; H_s = 2.0 m, T_p=5.5 s, direction 315 °N; H_s = 2.5 m, T_p=5.7 s, direction 315 °N and H_s = 3.0 m, T_p=6.0 s, direction 315 °N.

Basic processes

In unidirectional flow over a sand ridge the velocity profiles at both sides of the top of the ridge have a different shape; the velocity profiles upstream of the top of the ridge are characterized by increased velocities in the near-bed zone (bulgy shape due to decreasing water depth), while downstream of the top the velocity profiles are characterized by a dip (reduced velocities in the near-bed zone due to increasing water depth and deceleration processes), see Figure 3.

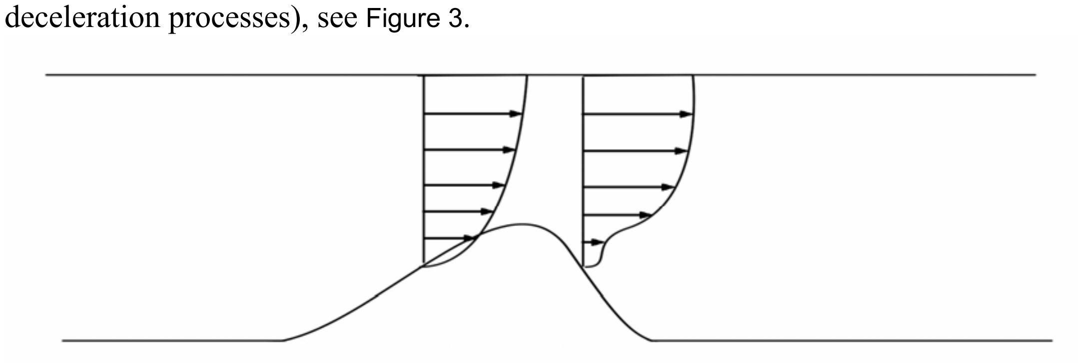

Figure 3. Velocity profiles over sand ridge

With tidal flow, the direction of the flow changes with the turning of the tide which has its consequences on the time-averaged velocity profiles at both sides of the ridge. At maximum flood and at maximum ebb, the velocity profiles show increased velocities at the upstream flank and show reduced near-bed velocities at the downstream flank. As the flow during flood and ebb is in opposite direction, the upstream and downstream locations are at opposite sides of the top; the bulgy velocity profiles change to dipped velocity profiles when the flow reverses. The time-averaged velocity profiles at both flanks show near-bed velocities as given in Figure 4 for the north flank and opposite for the south flank of the ridge. The time-averaged near-bed velocities on both flanks are in the direction of the top of the ridge.

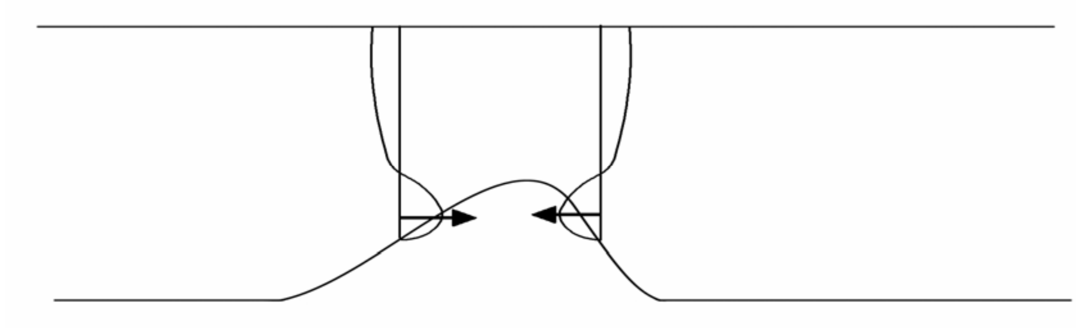

Figure 4. Time-averaged velocity profiles at flanks of the ridge

This mechanism results in vertical growth of the ridge when bed-load transport is dominant (particles remain in top region of the ridge). When suspended-load transport is dominant the particles may be transported beyond the top region resulting in flattening of the ridge. The tidal range with shallower water depths during ebb also affects velocities, transports and morphology. Herein, two important mechanisms, related to the shallower water depth during ebb, are discussed. The bed shear stress depends on water depth, as follows:

$$\vec{\tau}_b = \frac{g\rho\vec{U}\left|\vec{U}\right|}{C^2} \quad \text{and} \quad C = 18\log(\frac{12h}{k_s}) \qquad (2)$$

with: τ_b=bed shear stress [N/m^2]; g= gravitational acceralation [m/s^2]; ρ= water density [kg/m^3]; U=velocity [m/s]; C=Chézy coefficient [m$^{1/2}$/s]; k_s=equivalent roughness of Nikuradse [m].

The effect of waves also depends on the water depth. Waves intensify the stirring action of the fluid motion in the near-bed region which leads to larger sediment concentrations and larger transports; with shallower water the effect will be greater and transports will be larger. Thus with equal depth-averaged ebb- and flood-velocities, transports in ebb direction are larger than transports in flood direction due to wave action.

Model results for idealized ridge

Figure 5 shows the 5 year bottom profile development from simulations without waves using symmetric tides with velocity amplitudes of 0.50, 0.75 and 1.00 m/s. It can be seen that the ridge migrates in the ebb-direction. Furthermore it is found that the ridge increases in height for simulations with velocity amplitudes of 0.50 and 0.75 m/s and that the height is approximately unchanged with a velocity amplitude of 1.00 m/s. The latter simulation shows small boundary-related disturbances in morphology, which are not found from simulations with smaller velocity amplitudes. From this figure it is found that when suspended transport rates become significantly larger than the bed-load transport rates or when the suspended-load transport is not confined to the ridge vicinity only, the suspended-load transport dominates the effect of bed-load transport leading to flattening of the ridge height.